SPH-BASED SIMULATION OF MULTI-MATERIAL ASTEROID COLLISIONS

T.I. Maindl[1], C. Schäfer[2], R. Speith[3], Á. Süli[1,4], E. Forgács-Dajka[1,4], and R. Dvorak[1]

[1] *Institut für Astronomie, Universität Wien, Türkenschanzstraße 17, A-1180 Wien, Austria*
[2] *Institut für Astronomie und Astrophysik, Eberhard Karls Universität Tübingen, Auf der Morgenstelle 10, 72076 Tübingen, Germany*
[3] *Physikalisches Institut, Universität Tübingen, Auf der Morgenstelle 14, 72076 Tübingen, Germany*
[4] *Eötvös University, Department of Astronomy, 1518 Budapest, Pf. 32, Hungary*

Abstract   We give a brief introduction to smoothed particle hydrodynamics methods for continuum mechanics. Specifically, we present our 3D SPH code to simulate and analyze collisions of asteroids consisting of two types of material: basaltic rock and ice. We consider effects like brittle failure, fragmentation, and merging in different impact scenarios. After validating our code against previously published results we present first collision results based on measured values for the Weibull flaw distribution parameters of basalt.

1.   Introduction

Our goal is to investigate and explain the mechanisms of water delivery processes in early planetary systems. Existing dynamic studies simulate the behavior and collision statistics of asteroid families during and after the Late Heavy Bombardment in the early solar system (e.g., Dvorak et al. 2012) and assume a certain water content of the asteroids and complete water delivery to the impact target—usually a (proto)planet. By investigating the impact process itself we will get a more comprehensive description of water delivery starting at an even earlier point in planetary system evolution by answering the question: Under which circumstances

does water accumulate in or on bodies resulting from asteroid mergers rather than being lost during the impact?

The impact process can be simulated via a gravitationally bound rubble-pile model where gravitational reaccumulation of fragments governs the formation of (porous) bodies after disruptions (e.g., Richardson et al. 2000, 2009, 2012). Another approach is to directly simulate solid state mechanics during an impact. We follow the latter approach using smooth(ed) particle hydrodynamics (SPH) which is a meshless Lagrangian particle method and was developed by Lucy (1977) and Gingold and Monaghan (1977) for the simulation of compressible flows in astrophysical context. For a detailed description of SPH see, e.g., Monaghan (2005) or Schäfer et al. (2004). The method has been extended to solid state mechanics by Libersky & Petschek (1991). Additionally, a model for the simulation of brittle failure has been added by Benz & Asphaug (1994, henceforth referred to as BA94, and 1995). Impacts involving agglomerates such as protoplanetesimals and comets have been successfully simulated using porosity models as described in Schäfer, Speith & Kley (2007), Jutzi, Benz & Michel (2008) and Jutzi et al. (2009). Also, self gravity has been incorporated successfully. This makes SPH a promising tool for simulating planetary and asteroid dynamics (cf. Benavidez et al. 2012 and references therein). While typical grid codes are very well suited to hydrodynamics in protoplanetary discs they are not so well suited to treat elasto-plastic behavior or brittle failure which are important phenomena in collisions of asteroid-like (cf. Benz & Asphaug 1999, henceforth referred to as BA99, Michel, Benz & Richardson 2004) or moon-sized objects (Jutzi & Asphaug 2011).

Being a Lagrangian particle method, SPH is suitable for complex geometries of solid bodies. The continuum of the solid body is discretized into mass packages which are commonly referenced as particles. These particles interact by kernel interpolation and exchange momentum and energy (cf. Schäfer 2005). In this first study we introduce the basis of our parallel SPH code and state numerical tests and a first application.

2. Physical model

For modeling the solid bodies we use the Tillotson (1962) equation of state (EOS) as formulated in Melosh (1989). There are two domains depending upon the material energy density E. In the case of compressed regions ($\rho \geq \rho_0$) and E lower than the energy of incipient vaporization E_{iv} the EOS reads

$$P = \left[a + \frac{b}{1 + E/(E_0\eta^2)}\right]\rho E + A\mu + B\mu^2 \qquad (1)$$

with $\eta = \rho/\rho_0$ and $\mu = \eta - 1$. We denote pressure, density, and energy density by P, ρ, and E, respectively. The symbols ρ_0, A, B, E_0, a, and b are material constants. In case of an expanded state (E greater than the energy of complete vaporization E_{cv}) the EOS reads

$$P = a\rho E + \left[\frac{b\rho E}{1 + E/(E_0\eta^2)} + \frac{A\mu}{e^{\beta(\rho_0/\rho-1)}} \right] e^{-\alpha(\rho_0/\rho-1)^2} \qquad (2)$$

with two more material parameters α and β. In the partial vaporization regime $E_{\mathrm{iv}} < E < E_{\mathrm{cv}}$, P is linearly interpolated between the pressures obtained via (1) and (2), respectively. For a more detailed description see Melosh (1989).

The theory of continuum mechanics provides the equations for the conservation of mass, momentum and energy which describe the dynamics of a solid body (cf. e.g., Schäfer, Speith & Kley 2007). The conservation of mass is given by the continuity equation which reads in Lagrangian representation (Einstein notation)

$$\frac{\mathrm{d}\rho}{\mathrm{d}t} + \rho \frac{\partial v^\alpha}{\partial x^\alpha} = 0.$$

The equation for the conservation of momentum is

$$\frac{\mathrm{d}v^\alpha}{\mathrm{d}t} = \frac{1}{\rho} \frac{\partial \sigma^{\alpha\beta}}{\partial x^\beta}, \quad \sigma^{\alpha\beta} = -P\delta^{\alpha\beta} + S^{\alpha\beta}$$

with the stress tensor $\sigma^{\alpha\beta}$ given by the pressure P and the deviatoric stress tensor $S^{\alpha\beta}$ and $\delta^{\alpha\beta}$ denoting the Kronecker delta. Energy conservation reads

$$\frac{\mathrm{d}E}{\mathrm{d}t} = -\frac{P}{\rho} \frac{\partial v^\alpha}{\partial x^\alpha} + \frac{1}{\rho} S^{\alpha\beta} \dot{\epsilon}^{\alpha\beta}$$

with the strain rate tensor $\dot{\epsilon}^{\alpha\beta}$ given in (3).

In order to describe the dynamics of a solid body we have to specify the time evolution of the deviatoric stress tensor $S^{\alpha\beta}$. We use Hooke's law and define the time evolution as

$$\frac{\mathrm{d}S^{\alpha\beta}}{\mathrm{d}t} = 2\mu \left(\dot{\epsilon}^{\alpha\beta} - \frac{1}{3} \delta^{\alpha\beta} \dot{\epsilon}^{\gamma\gamma} \right) + S^{\alpha\gamma} R^{\gamma\beta} - R^{\alpha\gamma} S^{\gamma\beta},$$

where μ denotes the shear modulus. The last two terms involve the rotation rate tensor R and are rotation terms that are needed since the constitutive equations have to be independent from the material frame of reference. We apply the commonly used Jaumann rate form for the

Table 1. Characteristics of the code tests. The projectile is represented as one SPH particle in all cases.

Scenario #	Number of target particles	Target radius (m)	Impact velocity (m/s)	Impact angle (°)
T1	145,196	$3 \cdot 10^{-2}$	$3.2 \cdot 10^{3}$	30
T2	41,244	$3 \cdot 10^{-2}$	$3.2 \cdot 10^{3}$	30
T3	10,585	$3 \cdot 10^{-2}$	$3.2 \cdot 10^{3}$	30

rotation terms. The rotation rate and strain rate tensors are given by

$$R^{\alpha\beta} = \frac{1}{2}\left(\frac{\partial v^{\alpha}}{\partial x^{\beta}} - \frac{\partial v^{\beta}}{\partial x^{\alpha}}\right), \dot{\epsilon}^{\alpha\beta} = \frac{1}{2}\left(\frac{\partial v^{\alpha}}{\partial x^{\beta}} + \frac{\partial v^{\beta}}{\partial x^{\alpha}}\right). \tag{3}$$

This set of equations describes the dynamics of an elastic solid body. In order to model plastic behavior we follow the approach by BA94 and use the von Mises yield criterion where the deviatoric stress is limited depending on the material yield stress Y. We implement this by using a transformed deviatoric stress $S_{\text{vM}}^{\alpha\beta}$ according to

$$S_{\text{vM}}^{\alpha\beta} = \min\left[\frac{2\,Y^2}{3\,S^{\alpha\beta}S^{\alpha\beta}}, 1\right] \cdot S^{\alpha\beta}.$$

As basalt is a brittle material we additionally include a damage model for tensile failure. Physically, fracture is related to the failure of atomic or molecular bonds. In analogy to the continuum model for solid bodies a continuum model for fragmentation can be derived (Grady & Kipp 1980) and has been implemented for these simulations following the ansatz for SPH by BA94. The distribution $n(\epsilon)$ of flaws activated by a strain level of ϵ among the SPH particles is given by a Weibull distribution with material parameters k and m according to $n(\epsilon) = k\epsilon^{m}$.

3.   Scenarios

3.1   Code test

To validate our code we use impact simulation results of a lucite bullet impacting a spherical basalt target as published in BA94. We mimic their setup by using the Tillotson equation of state with parameters for basalt and lucite, the material and fracture model constants according to the published values, and only allowing the target to fracture.

In Tab. 1 we list the simulation characteristics of the code tests. Comparing our results demonstrated in Fig. 1 with the results of BA94 (cf. their Fig. 6) we see a high degree of agreement largely independent from
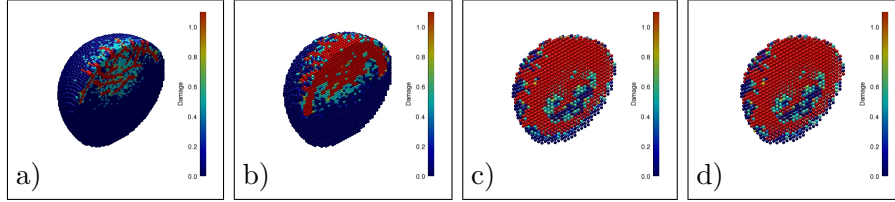
Figure 1. The damage pattern in the test case. The target is split in half to reveal the interior. Scenarios and time after the impact: a) T1, $9.0\,\mu$s, b) T2, $10.0\,\mu$s, c) T3, $25\,\mu$s, d) T3, $40\,\mu$s.
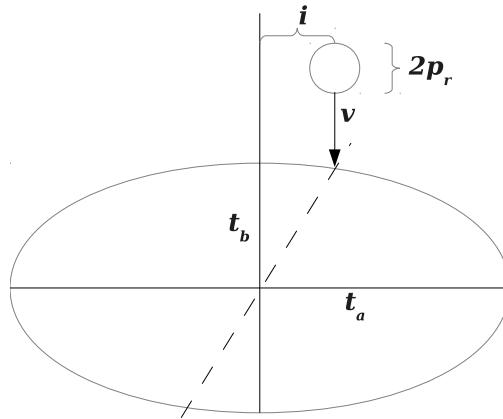

Figure 2. The impact geometry (projection onto the xy-plane), see text for details.

the number of particles used in the simulations. Note the cracks on the surface and the developing subsurface spherical damage patterns as demonstrated in Fig. 1 a–c which are consistent with Fig. 6 in the reference paper. Also apparent are only minimal changes after about $25\,\mu$s after the impact (Fig. 1 c and d).

3.2   Impact scenario

Our first simulations use a spheroidal target and a smaller, spherical projectile. We allow fracture in both the target and projectile which are composed of different materials.

We treat the collisions from a pure continuum mechanics point of view, i.e., we neglect self gravity as validated for time frames immediately following the impact by BA99.

As materials for the impacting bodies we use basalt (target) and water ice (projectile). Basalt is a widely adopted material in simulating aster-

Table 2. Tillotson EOS parameters, vaporization energy levels, shear modulus μ, and yield stress Y in SI units, cf. Benz & Asphaug (1999). Note that $A = B$ is set equal to the bulk modulus.

	ρ_0 (kg/m^3)	A (GPa)	B (GPa)	E_0 (MJ/kg)	E_{iv} (MJ/kg)	E_{cv} (MJ/kg)
Basalt	2700	26.7	26.7	487	4.72	18.2
Ice	917	9.47	9.47	10	0.773	3.04

	a	b	α	β	μ (GPa)	Y (GPa)
Basalt	0.5	1.50	5.0	5.0	22.7	3.5
Ice	0.3	0.1	10.0	5.0	2.8	1

oid collisions using both SPH (cf. for example Benavidez et al. 2012, BA99) and fluid dynamics codes (cf. Korycansky et al. 2006).

Figure 2 describes the geometry of the impact scenario: we use a spheroidal target with semi-axes $t_a = 10\,\mathrm{m}$ and $t_b = 5\,\mathrm{m}$ and a spherical projectile (radius $p_r = 1\,\mathrm{m}$) which impacts the target at a speed of $v = 1\,\mathrm{km/s}$ and an impact parameter $i = 3\,\mathrm{m}$. The initial particle distribution is chosen such that the projectile and target are composed of 154 and 38,776 SPH particles corresponding to projectile and target masses of about 3.813 and $2.827 \cdot 10^3$ tons, respectively.

We use the Tillotson EOS adopting the values given in BA99 following their reasoning on approximating ρ_0, setting A equal to the bulk modulus, and $B=A$ (see Tab. 2). From the same source we use the shear modulus μ and yield stress Y. Young's modulus E is given by $E = 9A\mu/(3A + \mu)$.

Similar to the situation with the EOS parameters, it is not easy to get publicly published parameter values for the Weibull distribution governing the density number of flaws. If measurements are not available for the respective material impact experiments can be simulated with varying Weibull parameter values followed by choosing the set of parameters best fitting the experimental results. As this is not entirely satisfactory we decided to use directly measured values for basalt $m_{basalt} = 16$, $k_{basalt} = 10^{61}\,\mathrm{m}^{-3}$ (Nakamura, Michel & Setoh 2007). For ice we adopt the values mentioned in Lange, Ahrens & Boslough (1984), $m_{ice} = 9.1$, $k_{ice} = 10^{46}\,\mathrm{m}^{-3}$.

Corresponding to the test results we present the evolving damage pattern of our simulations as 3D plots of targets split in half to reveal the inner structure. The cutting plane is aligned with the location of the impact and the origin as sketched by the dashed line in Fig. 2.
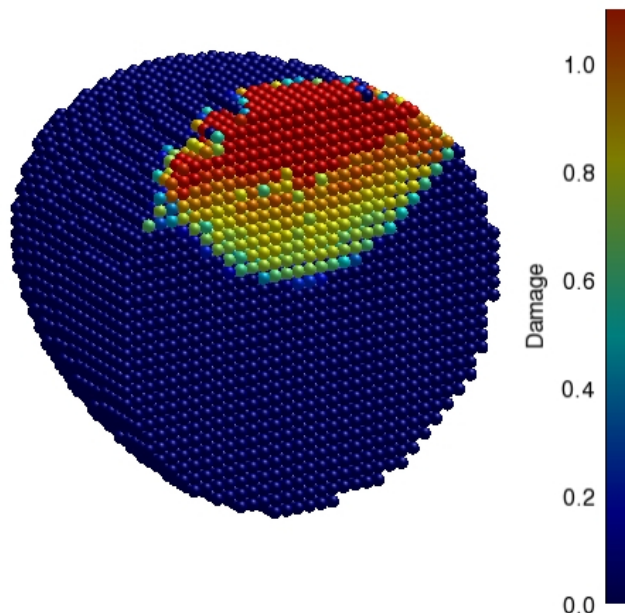
Figure 3. The damage pattern 0.6 ms after the impact.

As can be seen in Figs. 3 and 4, substantial subsurface damage as well as cracks in the surface develop, which is similar to the test scenario. Due to the massive projectile however, the core of the target is also destroyed and only a shell containing undamaged material remains. The surface pattern of undamaged areas intersected by cracks seems to be stable, though as indicated by the comparison of the overall picture 3 ms and 84 ms after the impact in Fig. 5. The developing inner damage structure will be subject to future higher-resolution simulations.

4. Conclusions and future research

We demonstrated and validated a new SPH code for continuum mechanics with a focus on collisions of bodies in early planetary systems. An immediate application will be connecting to close encounters and collisions as witnessed in n-body simulations (cf. Süli 2013). From investigating many such encounters we expect to get statistically significant results regarding the merging and fragmentation assumptions in various impact scenarios (velocities, angles, impact parameters, material composition, porosity, body shapes, etc.)—it is more the overall picture than high-accuracy single simulations that are of interest to us at the moment.
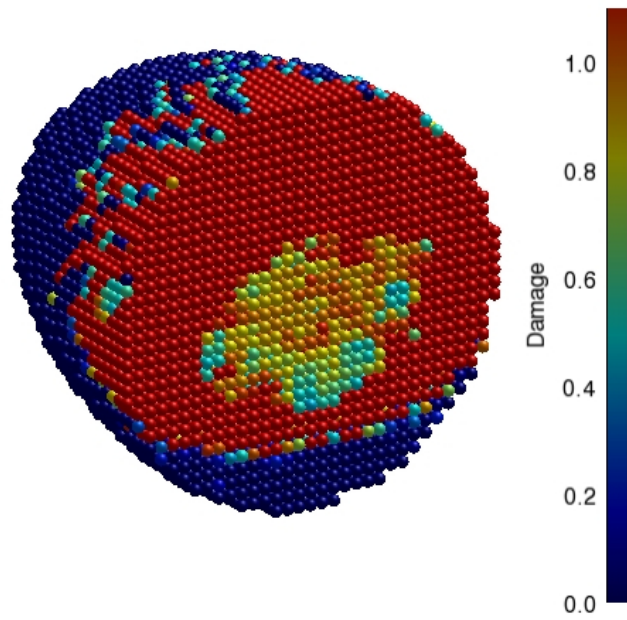
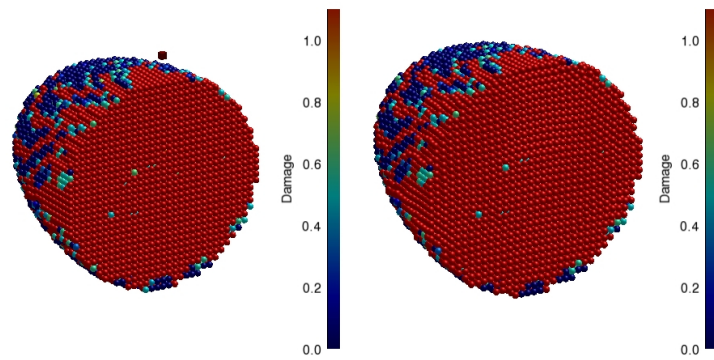*Figure 4.* The damage pattern 1.5 ms after the impact.

Figure 5. The damage patterns 3 ms (left) and 84 ms (right) after the impact.

Therefore a new, highly parallel code is a necessity to achieve significant results in reasonable computation time. Among others features like XSPH, tensile instability fixes, tensorial correction, artificial viscosity, damage limiting schemes, etc. can be adapted for the specific collision scenario under consideration.

Acknowledgments

References

Benavidez, P.G., Durda, D.D., Enke, B.L., Bottke, W.F., Nesvorný, D., Richardson, D.C., Asphaug, E., Merline, W.J.: 2012, Icar 219, 57

Benz, W., Asphaug, E.: 1994, Icar 107, 98

Benz, W., Asphaug, E.: 1995, CoPhC 87, 253

Benz, W., Asphaug, E.: 1999, Icar 142, 5

Dvorak, R., Eggl, S., Süli, Á., Sándor, Z., Galiazzo, M., Pilat-Lohinger, E.: 2012, AIP Conf. Proc. 1468, 137

Gingold, R.A., Monaghan, J.J.: 1977, MNRAS 181, 375

Grady, D.E., Kipp, M.E.: 1980, Int. J. Rock Mech. Min. Sci. Geomech. Abstr. 17, 147

Jutzi, M., Asphaug, E.: 2011, Natur 476, 69

Jutzi, M., Benz, W., Michel, P.: 2008, Icar 198, 242

Jutzi, M., Michel, P., Hiraoka, K., Nakamura, A.M., Benz, W.: 2009, Icar 201, 802

Korycansky, D.G., Harrington, J., Deming, D., Kulick, M.E.: 2006, ApJ 646, 642

Lange, M.A., Ahrens, T.J., Boslough, M.B.: 1984, Icar 58, 383

Libersky, L.D., Petschek, A.G.: 1991, LNP 395, 248

Lucy, L.B.: 1977, AJ 82, 10134

Melosh, H.J.: 1989, Impact Cratering: A Geologic Process (New York: Oxford Univ. Press)

Michel, P., Benz, W., Richardson, D.C.: 2004, P&SS 52, 1109

Monaghan, J.J.: 2005, RPPh 68, 1703

Nakamura, A.M., Michel, P., Setoh, M.: 2007, JGRE 112, E02001

Richardson, D.C., Quinn, T., Stadel, J., Lake, G.: 2000, Icar 143, 45

Richardson, D.C., Michel, P., Walsh, K.J., Flynn, K.W.: 2009, P&SS 57, 183

Richardson, D.C., Munyan, S.K., Schwartz, S.R., Michel, P.: 2012, LPSC 43.2195

Schäfer, C.: 2005, Dissertation, Eberhard-Karls-Universität Tübingen, Germany

Schäfer, C., Speith, R., Hipp, M., Kley, W.: 2004, A&A 418, 325

Schäfer, C., Speith, R., Kley, W.: 2007, A&A 470, 733

Süli, Á.: 2013, AN, in preparation

Tillotson, J.H.: 1962, General Atomic Report GA-3216

Weibull, W.A.: 1939, Ingvetensk. Akad. Handl. 151, 5